LA-UR- 09-00707

Approved for public release;
distribution is unlimited.

Title:	Transition from Collisional to Kinetic Reconnection in Large-Scale Plasmas
Author(s):	William Daughton, X-1-PTA Vadim Roytershteyn, T-15 Brian J. Albright, X-1-PTA Homa Karimabadi, UCSD Lin Yin, X-1-PTA Kevin Bowers, X-1-PTA
Intended for:	submitted to Physical Review Letters February 11, 2009

Los Alamos
NATIONAL LABORATORY
EST.1943

Form 836 (7/06)

Transition from Collisional to Kinetic Reconnection in Large-Scale Plasmas

W. Daughton[1], V. Roytershteyn[1], B. J. Albright[1], H. Karimabadi[2], L. Yin[1], and Kevin J. Bowers[1*]
[1] *Los Alamos National Laboratory, Los Alamos, NM 87544*
[2] *University of California, San Diego, La Jolla, 92093*
(Dated: February 4, 2009)

Using first-principles fully kinetic simulations with a Fokker-Planck collision operator, it is demonstrated that Sweet-Parker reconnection layers are unstable to a chain of plasmoids (secondary islands) for Lundquist numbers beyond $S \gtrsim 1000$. The instability is increasingly violent at higher Lundquist number, both in terms of the number of plasmoids produced and the super-Alfvénic growth rate. A dramatic enhancement in the reconnection rate is observed when the half-thickness of the current sheet between two plasmoids approaches the ion inertial length. During this transition, the reconnection electric field rapidly exceeds the runaway limit, resulting in the formation of electron-scale current layers that are unstable to the continual formation of new plasmoids.

PACS numbers: 52.35.Vd, 52.35.Py, 52.65.-y

The conversion of magnetic energy into kinetic energy through the process of magnetic reconnection remains one of the most challenging and far reaching problems in plasma physics. One key issue is the scaling of the reconnection dynamics for applications where the system size is vastly larger than the kinetic scales. The magnetohydrodynamics (MHD) model should provide an accurate description of *collisional* reconnection where the resistive layers are larger than the ion kinetic scale. For uniform resistivity, MHD gives rise to the Sweet-Parker (SP) model in which the rate scales as $U_{in}/V_A \approx \delta_{sp}/L_{sp} \approx S^{-1/2}$ where U_{in} is the inflow velocity, $V_A = B/\sqrt{4\pi m_i n}$ is Alfvén velocity, δ_{sp} is the half-thickness and L_{sp} is the half-length of the layer, $S = 4\pi V_A L_{sp}/\eta c^2$ is the Lundquist number and η is the resistivity. Assuming that L_{sp} scales with the system size, implies $S \sim 10^6 - 10^{14}$ for many applications. Since the resulting dissipation rates are much slower than observations, *collisional* is often used synonymously to denote *slow* reconnection.

Surprisingly, there is a fundamental flaw with these arguments that is not widely appreciated. While the SP scaling is well verified with MHD simulations for $S \lesssim 2000$, at higher Lundquist numbers the elongated SP layers are unstable to plasmoid formation [1–3]. Recent linear theory [4] predicts a growth rate that scales as $S^{1/4} V_A/L_{sp}$ with the number of plasmoids increasing with $S^{3/8}$, indicating an increasingly violent instability for the relevant regimes. Performing the necessary simulations at high Lundquist remains an outstanding challenge, but recent results suggest this instability may lead to much faster turbulent reconnection [5].

Due to this instability, the scaling of *collisional* reconnection remains uncertain beyond $S \gtrsim 10^4$. Furthermore, the formation of plasmoids may rapidly lead to the breakdown of MHD when the new resistive layers between islands approach the ion kinetic scale. This regime is typically referred to as *kinetic* or *fast* reconnection since a variety of two-fluid and kinetic models predict rates that are weakly dependent on the system size and dissipation mechanism [6, 7] (the precise scalings are still a subject of controversy [8, 9]). In neutral sheet geometry, both two-fluid simulations [10, 11] and theory [12] predict an abrupt transition from the collisional to the kinetic regime when $\delta_{sp} \leq d_i$ where d_i is the ion inertial length. In this geometry, d_i is comparable to the ion gyroradius, and in the kinetic regime d_i is also comparable to the ion crossing orbit scale.

Recently, this transition between collisional and kinetic reconnection was proposed as the central mechanism in regulating coronal heating [13–15]. However, these estimates were based on the assumption of a stable SP layer within the collisional regime. To properly describe the dynamics at high Lundquist number, it is crucial to consider how plasmoid formation may influence the transition. To address this problem, this work employs fully kinetic particle-in-cell (PIC) simulations with a Monte-Carlo treatment [16] of the Fokker-Planck collision operator. For Lundquist numbers where the SP layers are stable $S \lesssim 1000$, this powerful first-principles approach has demonstrated a clear transition between the collisional and kinetic regimes near the expected threshold $\delta_{sp} \lesssim d_i$ [17]. Here we demonstrate that SP layers are increasingly unstable to plasmoid formation in large-scale systems. The observed growth rate is super-Alfvénic, allowing the islands to grow to large amplitude before they are convected downstream. A dramatic enhancement in the reconnection rate is observed when the current sheet between two plasmoids approaches the ion kinetic scale. During this transition, the reconnection electric field exceeds the runaway limit leading to a collapse of the diffusion region current sheet to the electron kinetic scale. These electron layers form elongated current sheets which are also unstable to the formation of new plasmoids in a manner similar to the collisionless limit [8, 18, 19].

*Guest Scientist. Currently with D. E. Shaw Research,LLC, New York, NY 10036.

The simulations were performed with the kinetic plasma simulation code VPIC [20] which has been modified to include Coulomb collisions and benchmarked carefully against transport theory [17]. The initial condition is a Harris sheet with magnetic field $B_x = B_o \tanh(z/\lambda)$ and density $n = n_o \mathrm{sech}^2(z/\lambda)$ provided by drifting Maxwellian distributions with uniform temperature $T_e = T_i = T_o$ ($\lambda = 2d_i$ is the half-thickness of the current sheet and B_o is the asymptotic field). A uniform non-drifting background is included with density $n_b = 0.3n_o$ and equal temperature. In order to reduce the large separation between electron and ion scales, it is necessary to employ an artificial mass ratio of $m_i/m_e = 40$. Other parameters are $\omega_{pe}/\Omega_{eo} = 2$ where $\omega_{pe} = \sqrt{(4\pi n_o e^2)/m_e}$ is the electron plasma frequency and $v_{the}/c = 0.35$ where $v_{the} = (2T_o/m_e)^{1/2}$ is the electron thermal speed. Lengths are normalized to the ion inertial scale $d_i = c/\omega_{pi}$ where $\omega_{pi} = \sqrt{(4\pi n_o e^2)/m_i}$ and time is normalized to the ion cyclotron frequency $\Omega_{io} = eB_o/(m_i c)$.

The Fokker-Planck treatment of Coulomb collisions gives rise to a number of complications not normally considered in the fluid calculations [17]. In neutral sheet geometry, the resistivity perpendicular to the magnetic field $\eta_\perp$ plays the dominant role in setting the structure of the SP layer, except for a small region near the x-point where the local electron cyclotron frequency falls below the electron-ion collision frequency ($\Omega_e < \nu_{ei}$). In this region, the resistivity approaches the unmagnetized Spitzer result. Furthermore, the resistivity varies in both space and time due to electron Ohmic heating within the layer. Working in dimensionless units, the perpendicular resistivity from transport theory [21] is

$$\hat{\eta}_\perp \equiv \frac{\omega_{pi}^2}{4\pi\Omega_{io}}\eta_\perp = \hat{\eta}_{\perp o}\left(\frac{T_o}{T_e}\right)^{3/2} , \qquad (1)$$

where T_e the local electron temperature and $\hat{\eta}_{\perp o} = 0.04$ is the initial resistivity for all simulations in this study. The coefficient $\hat{\eta}_{\perp o}$ is set by properly scaling ν_{ei} and the subsequent time evolution of $\hat{\eta}_\perp$ is well described [17] by (1) for parameter regimes in which the reconnection electric field E_y is small in comparison to the runaway limit $E_{cr} \approx (m_e T_e/2)^{1/2}\nu_{ei}/e$. Within the collisional SP regime, this ratio is approximately $E_y/E_{cr} \sim (d_i/\delta_{sp})(m_e/m_i)^{1/2}$, which implies that SP layers are always in a regime where (1) is valid. After the transition to the kinetic regime, the rapid increase in the reconnection rate can quickly lead to runaway fields $E_y > E_{cr}$ where (1) breaks down. While it is unclear how to model this within fluid theory, the approach in this manuscript is rigorously correct in both regimes.

The system sizes considered are summarized in Table I, along with the number of computational cells for each case, the initial Lundquist number S_o computed using $\hat{\eta}_{\perp o} = 0.04$ and the maximum Lundquist number S_{max} computed using $\hat{\eta}_\perp$ in the layer at the time of the transition. The time step for all simulations was $\Delta t\Omega_{ce} = 0.13$ with 1000 particles per cell to represent the plasma. The boundary conditions are periodic in the x-direction for both particles and fields while the z-boundaries are treated as conducting surfaces that elastically reflect particles.

TABLE I: Summary of parameters: System size L_x, cells N_x, Lundquist number $S_o \equiv 4\pi V_A L_{sp}/(\eta_{\perp o} c^2)$ based on the initial resistivity $\hat{\eta}_{\perp o} = 0.04$ and assuming $L_{sp} \approx L_x/4$, maximum Lundquist number S_{max} due to electron heating in the layer, predicted transition resistivity $\hat{\eta}_c$ required for $\delta_{sp} \approx d_i$, the actual resistivity $\hat{\eta}_\perp$ within the layer at the transition time τ, the number of plasmoids N_p within the SP layer and the transition time τ normalized to the Alfvén time $\tau_A = L_{sp}/V_a$. The transverse size is $L_z = 100d_i$ with 1600 cells for all cases.

L_x/d_i	N_x	S_o	S_{max}	$\hat{\eta}_c$	$\hat{\eta}_\perp$	N_p	τ/τ_A
100	1600	625	1140	0.04	0.025	0	-
200	3200	1250	2500	0.02	0.020	3	2.7
400	6400	2500	5000	0.01	0.019	4	1.8
800	12800	5000	11700	0.005	0.018	7	1.2

For periodic boundary conditions, simulations [11, 17] indicate the half-length of the SP layer is approximately $L_{sp} \approx L_x/4$ where L_x is the system size in the x-direction. Assuming the SP layer is stable, the two-fluid transition condition $\delta_{sp} \leq d_i$ may be re-expressed as

$$\hat{\eta}_\perp \leq \frac{d_i}{L_{sp}} \approx \frac{4d_i}{L_x} \equiv \hat{\eta}_c , \qquad (2)$$

where $\hat{\eta}_c$ is the critical transition resistivity. For the smallest simulation in Table I, this is equal to the initial resistivity while the larger simulations require increasing amounts of Ohmic heating in order to reduce the resistivity in the layer to this critical value.

The simulations are initiated with a small magnetic perturbation using the same functional form as Ref. [17] with magnitude $\delta B_z = 0.025B_o$. The reconnection rate is calculated from $E_R = \langle \partial\psi/\partial t \rangle / (BV_A)$, where $\psi = \max(A_y) - \min(A_y)$ along $z = 0$, A_y is the y-component of the vector potential, B and V_A are evaluated at $10d_i$ upstream of the dominant x-point and $\langle\ \rangle$ represents a time average over $\Delta t\Omega_{io} = \pm 5$ to reduce noise.

The resulting reconnection rates are shown in the top panel of Fig. 1 for the time interval $t\Omega_{io} = 0 \rightarrow 100$. As expected for the SP regime, the rates are progressively slower for the larger systems. Since the initial resistivity and sheet thickness are the same for all simulations, the time evolution of the electron temperature and resistivity are also quite similar. Thus the SP scaling prediction can be tested by plotting the average rate as function of $(d_i/L_x)^{1/2}$ as illustrated in the bottom panel. These results demonstrate that the collisional kinetic simulations have properly recovered the SP scaling.

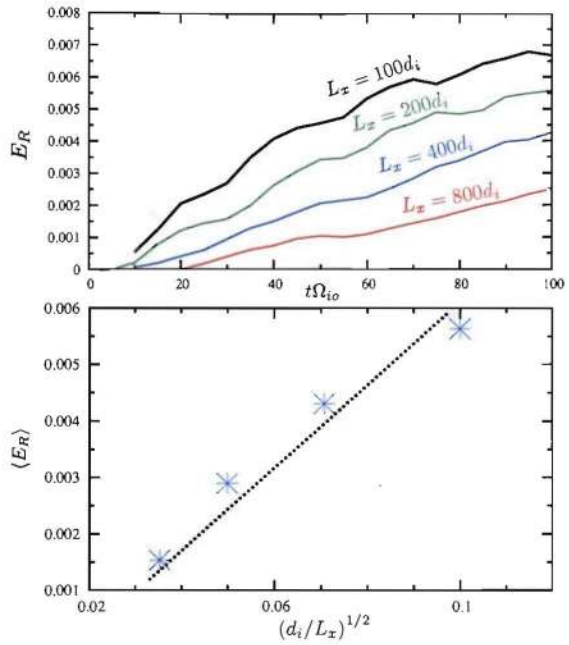

FIG. 1: Time evolution of the reconnection rates (top) at early time and the average reconnection rates over the interval $t\Omega_{io} = 40 \rightarrow 100$ as a function of $(d_i/L_x)^{1/2}$ (bottom).

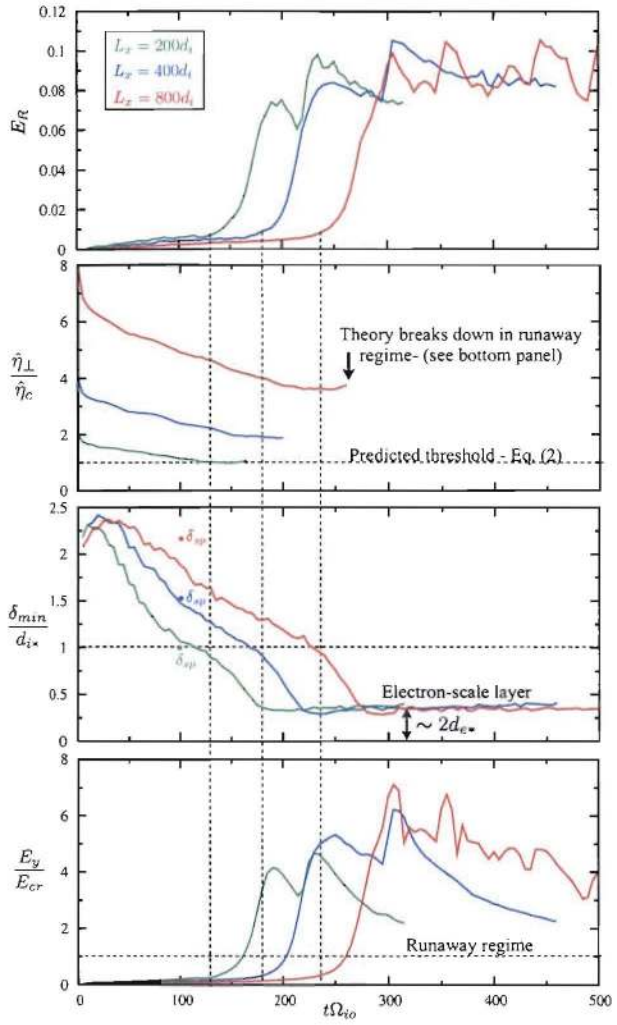

FIG. 2: Time evolution of the simulations in Table I showing the reconnection rate E_R, the perpendicular resistivity $\hat{\eta}_\perp$ implied by (1) normalized to the critical transition resistivity, the minimum current sheet thickness δ_{min} measured across the layer normalized to the local ion inertial scale d_{i*} computed using the actual density and the reconnection electric field E_y normalized by the runaway limit E_{cr}. The vertical lines denote the transition time τ where the abrupt increase in the rate is observed.

Over longer time scales, all simulations in Table I transition to much faster rates. The smallest $L_x = 100d_i$ simulation remains in a stable SP configuration until the half-thickness of the layer reaches the ion inertial length. In this case, the transition to the kinetic regime is very similar to the results described in Ref. [17]. Due to limited space, the rest of this letter is focused on the three largest cases in Table I. As illustrated in the top panel of Fig. 2, the reconnection rates increase dramatically near the transition times highlighted by the vertical dashed lines. In contrast to the early time evolution in Fig. 1, the average rates at late time actually *increase* slightly for the larger systems. To examine the transition condition (2), the second panel shows the evolution of the resistivity $\hat{\eta}_\perp$ normalized to the critical value $\hat{\eta}_c$ for each case. While the $L_x = 200$ case transitions near the expected threshold (2), the larger simulations transition sooner.

The reason for this discrepancy is that the SP layers are unstable to plasmoid formation while the simple estimate (2) assumes a stable SP layer. As summarized in Table I, the number of plasmoids observed in the SP layers near the transition time increases significantly with the Lundquist number, with a chain of 7 plasmoids for the largest case. To better illustrate the structural evolution, the current density J_y and flux surfaces are given in Fig. 3 for the $L_x = 800d_i$ case. During the initial evolution $t\Omega_{io} \lesssim 200$, the reconnection layer resembles the classic SP configuration as shown in the top panel. However, closer inspection reveals the initial growth of the instability at $t\Omega_{io} \sim 140$. The chain of plasmoids is clearly visible at $t\Omega_{io} \approx 250$ in the second panel.. These plasmoids break the SP layer into a series of separate reconnection sites with a current sheet between each island as illustrated in the third panel at $t\Omega_{io} \approx 300$.

In order to measure the scale of the various current layers during this complex evolution, a diagnostic was constructed to scan across the system in the x-direction 10 cells at time and measured the half-thickness of the current profile at each location. The minimum half-thicknes resulting from this procedure is denoted by δ_{min}. In the third panel of Fig. 2, δ_{min} is normalized to an ion inertial length d_{i*} based on the time evolving central density. Within the initial SP regime, δ_{min} is in reasonable

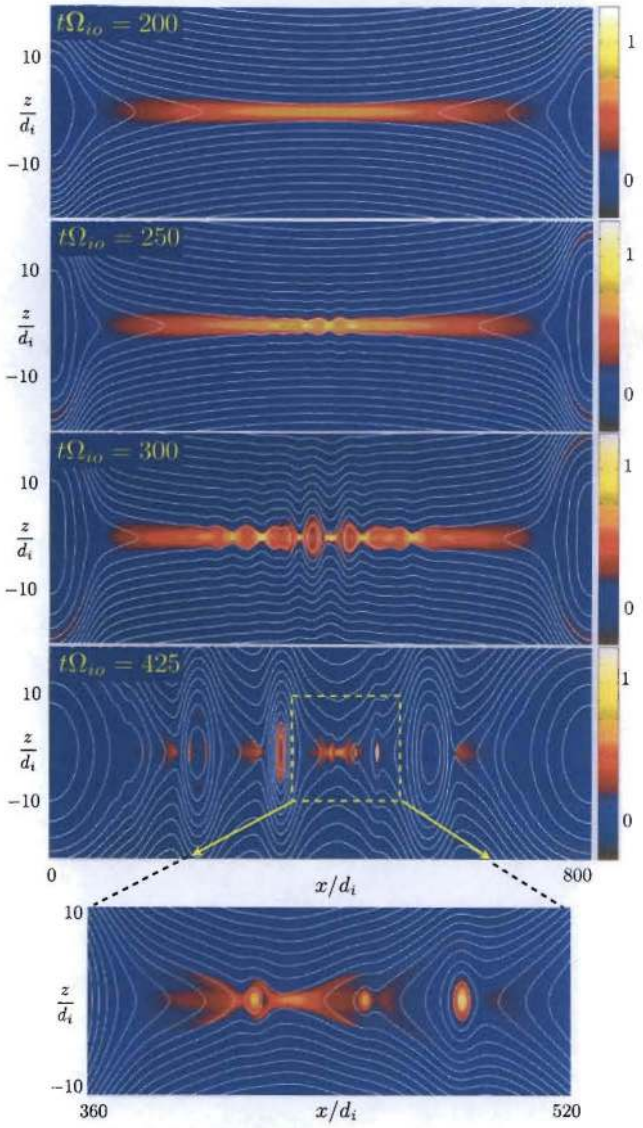

FIG. 3: Time evolution of the current density J_y for the largest $L_x = 800d_i$ simulation. White lines are the magnetic flux surfaces and the bottom panel is a close-up of the region indicated at $t\Omega_{io} = 425$ to illustrate the repeated formation of new plasmoids within the electron layer. The current density is normalized to the initial peak value $J_o = cB_o/(4\pi\lambda)$.

agreement with the theoretical SP thickness as indicated by the respective circles at $t\Omega_{io} \approx 100$ computed using $\delta_{sp}/d_{i*} \approx (L_{sp}\hat{\eta}_\perp/d_i)^{1/2}$. While the $L_x = 200d_i$ simulation is already near $\delta_{min} \approx d_i$, the other two simulations would not be expected to transition based on the observed electron heating (and reduction of resistivity). However, the growth of plasmoids leads to the intensification of the current density between the islands, and there is a dramatic increase in the reconnection rate when the thickness of these layers approach $\delta_{min} \approx d_{i*}$.

After the transition to the kinetic regime, the reconnection electric field greatly exceeds the runaway limit as illustrated in the bottom panel of Fig. 2. As a consequence, the diffusion region current sheet collapses to the electron scale $\delta_{min} \approx 2d_{e*}$. In this runaway regime, collisional momentum exchange is increasingly ineffective and the reconnection electric field is balanced predominantly by the divergence of the electron pressure tensor [17]. The resulting electron layers are unstable to the repeated formation of new plasmoids as illustrated in the bottom panel of Fig. 3. In this simulation, 6 new plasmoids are generated within the central electron layer leading to significant time modulations in the reconnection rate similar to recent collisionless simulations [8, 18, 19].

The first-principles kinetic simulations in this letter indicate that Sweet-Parker reconnection is unstable to plasmoid formation for Lundquist numbers larger than $S \gtrsim 1000$. Although it is difficult to infer reliable scalings from this limited study, the number of plasmoids in Table I increases roughly as $N_p \propto S^{0.6}$ while the onset time decreases $\tau/\tau_A \propto S^{-0.5}$. Although these trends are in the same direction as recent MHD theory [4], the specific scalings are stronger functions of S is the present kinetic simulations. Regardless of the precise scaling, these trends imply an increasingly violent instability at large S, with super-Alfvénic growth rates that permit the plasmoids to reach large amplitude before they are convected downstream by the Alfvénic outflow. As a result, new current sheets form between the islands that are significantly thinner than the overall SP layer. When the half-thickness of these layers approach the ion kinetic scale, there is a rapid increase in the reconnection rate as the dynamics transitions into the kinetic regime.

The results in this letter indicate that plasmoid formation plays a crucial role in determining the transition between collisional and kinetic regimes. The widely used transition condition (2) is relevant only for $S \lesssim 1000$ where SP layers are structurally stable. It may be possible to construct new estimates for the onset of kinetic reconnection, based on the scaling for the number of plasmoids $N_p \propto S^\alpha$ and assuming the length of the new current sheets scale as $\sim L_{sp}/N_p$. One could then compare the thickness of these new resistive layers with the ion kinetic scale.

We gratefully acknowledge the support of the U.S. Department of Energy through the LANL/LDRD Program for this work. Contributions from HK were supported by the NASA Heliophysics Theory Program.

[1] M. Yan, L. Lee, and E. Priest, J. Geophys. Res. **92**, 8277 (1992).
[2] F. Malara, P. Veltri, and V. Carbone, Phys. Fluids B **4**, 3070 (1992).
[3] D. Biskamp, Phys. Fluids **29**, 1520 (1986).
[4] N. F. Loureiro, A. A. Schekochihin, and S. C. Cowley, Phys. Plasmas **14** (2007).

[5] G. Lapenta, PRL **100**, 235001 (2008).
[6] J. Birn, J. Drake, M. Shay, B. Rogers, R. Denton, M. Hesse, M. Kuznetsova, Z. Ma, A. Bhattacharjee, A. Otto, et al., J. Geophys. Res. **106**, 3715 (2001).
[7] M. Shay, J. Drake, B. Rogers, and R. Denton, J. Geophys. Res. **106**, 3759 (2001).
[8] W. Daughton, J. Scudder, and H. Karimabadi, Phys. Plasmas **13**, 072101 (2006).
[9] A. Bhattacharjee, K. Germaschewski, and C. Ng, Phys. Plasmas **12**, 042305 (2005).
[10] Z. Ma and A. Bhattacharjee, Geophys. Res. Lett. **23**, 1673 (1996).
[11] P. Cassak, M. Shay, and J. Drake, Phys. Rev. Lett. **95**, 235002 (2005).
[12] A. N. Simakov and L. Chacón, Phys. Rev. Lett **101**, 105003 (2008).
[13] P. Cassak, J. Drake, and M. Shay, Astrophys. J. **644**, L145 (2006).
[14] D. Uzdensky, Astrophys. J. **671**, 2139 (2007).
[15] D. Uzdensky, Phys. Rev. Lett. **99**, 261101 (2007).
[16] T. Takizuka and H. Abe, J. Comput. Phys. **25**, 205 (1977).
[17] W. Daughton, V. Roytershteyn, B. Albright, H. Karimabadi, L. Yin, and K. J. Bowers, Phys. Plasmas **submitted** (2009).
[18] H. Karimabadi, W. Daughton, and J. Scudder, Geophys. Res. Lett. **34**, L13104 (2007).
[19] A. Klimas, M. Hesse, and S. Zenitani, Phys. Plasmas **15**, 082102 (2008).
[20] K. J. Bowers, B. J. Albright, L. Yin, B. Bergen, and T. J. T. Kwan, Phys. Plasmas **15**, 055703 (2008).
[21] S. Braginskii, Reviews of Plasma Physics **1**, 205 (1965).